Food & Function

ROYAL SOCIETY OF CHEMISTRY

PAPER

View Article Online
View Journal | View Issue

Cite this: *Food Funct.*, 2026, **17**, 2955

Systematic evaluation of permeability-related behavior and physicochemical determinants of structurally diverse phytochemicals using a Caco-2 cell model

Rixing Cong,[a] Jin-Woo Kim,[a] Jun-Su Park,[b] Jin-Soo Park,[b,c] Kyungsu Kang [b,c] and Soon-Mi Shim *[a]

Understanding the intestinal permeability of phytochemicals is essential for elucidating their bioavailability and physiological efficacy. This study systematically investigated 162 structurally diverse phytochemicals across 15 chemical classes using the human intestinal Caco-2 cell monolayer model. Transepithelial electrical resistance (TEER), apparent permeability coefficients (P_{app}), and efflux ratios (ER) were determined to evaluate barrier integrity, passive diffusion, and transporter-mediated efflux, respectively. TEER responses ranged from 44.4 ± 0.5% to 138.8 ± 10.2% across the 162 compounds, indicating both barrier-disruptive and barrier-enhancing effects depending on compound structure. Apparent permeability coefficients (P_{app}, AP → BL) spanned 0.11 ± 0.13 × 10^{-6} to 129.0 ± 6.6 × 10^{-6} cm s^{-1}, demonstrating large variability across classes. Among these, alkaloids, benzopyrans, flavonoids, and phenolic compounds exhibited the highest permeability, whereas ginsenosides, polysaccharides, and polypeptides were largely undetectable. P_{app} and recovery values correlated positively with lipophilicity (X log P) but negatively with topological polar surface area (TPSA) and hydrogen bonding capacity (HBD, HBA). Principal component analysis (PCA) integrating physicochemical and permeability-related variables explained 63.8% of total variance and illustrated overall multivariate associations among variables. PCA was used as an exploratory visualization tool and suggested that permeability-related parameters were associated with lipophilicity and molecular polarity rather than chemical class alone. These observations provide descriptive insight into structure–permeability relationships but should be interpreted in conjunction with direct permeability measurements.

Received 24th November 2025,
Accepted 1st March 2026

DOI: 10.1039/d5fo05099e

rsc.li/food-function

Introduction

Bioavailability refers to the extent and rate at which an active substance is absorbed into the bloodstream and becomes available at the site of action.[1,2] Previous studies have shown that the physiological efficacy of a nutrient or bioactive compound is more closely related to its bioavailable concentration than to its total intake.[3] In this context, evaluating the bioavailability of natural compounds is essential for understanding their potential health benefits and for the development of effective functional ingredients or therapeutic agents.[4,5] Systematic characterization of diverse natural products enables comparative analysis of absorption and metabolic behavior and facilitates the establishment of a reference dataset for identifying and classifying physiologically active molecules.[6–9]

Phytochemicals possess diverse structural and physicochemical properties, which enable them to exhibit a wide range of biological activities.[10] For instance, alkaloids, characterized by basic nitrogen atoms, are classified into heterocyclic and non-heterocyclic forms and exhibit neuroprotective, anticancer, and antibacterial activities.[11,12] Amino acids, as the building blocks of proteins, play essential roles in biosynthetic pathways and the regulation of oxidative stress, immunity, and metabolic disorders.[13,14] Benzopyrans, including tocotrienols (members of the chroman/benzodihydropyran subgroup), feature a fused aromatic and oxygen-containing ring and exhibit antioxidant and cardioprotective properties.[15,16] Cinnamic acid derivatives, a major class of phenylpropanoid compounds, are known for their glucose-regulating and anti-inflammatory effects.[17,18] Flavonoids, a major class of polyphe-

[a]*Department of Food Science and Biotechnology, Sejong University, 209, Neungdong-ro, Gwangjin-gu, 05006 Seoul, Republic of Korea. E-mail: soonmishim@sejong.ac.kr; Fax: +82-2-3408-4319; Tel: +82-2-3408-3229*
[b]*Center for Natural Product Systems Biology, KIST Gangneung Institute of Natural Products, Gangneung 25451, Republic of Korea*
[c]*Natural Product Applied Science, KIST School, University of Science and Technology, Gangneung 25451, Republic of Korea*

nols characterized by a diphenylpropane (C6–C3–C6) skeleton, are recognized for their antioxidant capacity and cardiovascular benefits, largely due to their conjugated structures.[19,20] Ginsenosides, triterpene saponins found in ginseng, and glycosides, composed of a sugar moiety linked to an aglycone, both exhibit a wide range of bioactivities including neuroprotection and metabolic regulation.[21,22] Additional classes, such as polypeptides, phenolic compounds, quinones, polysaccharides, steroids, and terpenoids, further highlight the structural diversity and broad biological functions of natural compounds, ranging from antioxidants and immunomodulatory effects to anti-inflammatory and antimicrobial activities.[23–28]

By encompassing compounds with varying physicochemical properties and molecular complexities, this study aims to provide a deeper understanding of the absorption characteristics of phytochemicals. Such a broad-spectrum analysis is expected to enhance the predictive power of *in vitro* models and support the rational design and utilization of bioactive compounds in functional foods and therapeutic applications. The present study assessed the key indicators for phytochemical bioavailability such as apparent permeability (P_{app}), TEER, efflux ratio (ER) by using the Caco-2 cell model, a widely accepted *in vitro* model for intestinal absorption in combination with high performance liquid chromatography (HPLC) – ultraviolet (UV) or – evaporative light scattering detector (–ELSD) analysis. The Caco-2 cell model is widely employed as an *in vitro* system for evaluating intestinal permeability of pharmaceutical and dietary compounds due to its ability to mimic key features of the human intestinal epithelial barrier.[29] However, this model does not fully reproduce the complexity of *in vivo* intestinal absorption, such as the influence of metabolic processes, transporter activity, and physiological dynamics.[29] Therefore, data obtained from Caco-2 permeability experiments should be interpreted as comparative *in vitro* indicators of intestinal permeability rather than direct quantitative predictors of *in vivo* bioavailability. Given the enormous chemical diversity of phytochemicals, this study focused on a curated, analysis-ready library rather than an exhaustive collection. We selected 162 phytochemicals including alkaloids, terpenoids, benzopyrans, cinnamic acids, flavonoids, ginsenosides, glycosides, polypeptides, quinones, polysaccharides, phenolic compounds, amino acids as well as less common structural types such as ketones, diazolidines, phenazines, and pyrazolones according to predefined criteria: (i) availability and completeness of the target experimental endpoints and core metadata, (ii) unambiguous structural identifiability (*e.g.*, unique identifiers/SMILES) required for molecular descriptor computation, and (iii) representativeness across major phytochemical families to cover a wide chemical space. Compounds lacking sufficient endpoint information, presenting inconsistent records, or appearing as duplicates (*e.g.*, synonyms/salts recorded multiple times) were removed. This curation strategy balances chemical diversity with data quality and feasibility, thereby supporting robust downstream analysis and model development.

Materials and methods

Chemicals and reagents

The analytical standards of (−)-cytisine, (−)-dihydroquinine, (+)-bicuculline, (+)-nootkatone, (+)-taxifolin, (+)-usnic acid, (±)-evodiamine, (*E*)-3-(4-chlorophenyl)acrylic acid, (*E*)-cinnamyl alcohol, (*S*)-(+)-camptothecin, 2-(2-hydroxyethyl)phenol, 2-(4-hydroxyphenyl)ethanol, 20(*R*)-ginsenoside Rg2, 20(*R*)-ginsenoside Rh1, 20(*S*)-ginsenoside Rg3, 20-*O*-glucoginsenoside Rf, 3-(3,4-dihydroxyphenyl)-L-alanine, 3,5-dimethoxy-4-hydroxycinnamic acid, 3-methyl-1-phenyl-2-pyrazoline-5-one, 4′,6,7-trihydroxyisoflavone, 4-formylphenyl β-D-allopyranoside, 4′-hydroxy-3′-methoxyacetophenone, abietic acid, aegeline, allantoin, amygdalin, andrographolide, arbutin, atropine, bacitracin, baicalin, berberine chloride hydrate, bergapten, bergenin, betulin, bisdemethoxycurcumin, boldine, brucine hydrate, capsaicin (natural), carminic acid (natural dye), cepharanthine, cholecalciferol, chrysazin, colchicine, compound **K**, cromolyn sodium salt, curcumin (natural), curcumin (synthetic), cycloheximide, digoxin, ellagic acid, ellagic acid dihydrate, ergosterol, galantamine hydrobromide, ginsenoside F1, ginsenoside F2, ginsenoside F3, ginsenoside F4, ginsenoside F5, ginsenoside Rb1, ginsenoside Rb2, ginsenoside Rb3, ginsenoside Rc, ginsenoside Rd, ginsenoside Re, ginsenoside Rf, ginsenoside Rg1, ginsenoside Rg2, ginsenoside Rg4, ginsenoside Rg5, ginsenoside Rh1, ginsenoside Rh2, ginsenoside Rk3, glycyrrhetic acid, glycyrrhizin, gramicidin (mixture of **A**, **B**, **C** and **D**), gramine, griseofulvin, gypenoside A, gypenoside L, gypenoside XLIX, gypenoside XVII, harmine, harmol, hecogenin, hematoxylin hydrate, hesperidin, hinokitiol, icariin, indican, jatrorrhizine chloride, khellin, lanatoside C, LDN-22684, limonin, L-tetrahydropalmatine, lycorine, magnolol, mangiferin, matrine, mollugin, nordihydroguaiaretic acid, noscapine hydrochloride hydrate, notoginsenoside Fe, notoginsenoside Ft1, notoginsenoside R1, notoginsenoside R2, oleuropein, oridonine, paeoniflorin, papaverine hydrochloride, parthenolide, phenazine methosulfate, phenethyl caffeate, piceid, pilocarpine hydrochloride, piperine, piperlongumine, protopanaxatriol, punicalagin, purpurin, quinidine, rebaudioside A, reserpine, resveratrol, rhaponticin, rhododendrol, rosmarinic acid, rotenone, rutaecarpine, salicin, *S*-allyl-L-cysteine, santonin, sclareol, scopolamine hydrobromide trihydrate, sesamin, sesamol, sinigrin, stevioside, swertiamarin, synephrine, tabersonine, tanshinone IIA, tetrahydropalmatine, tetrandrine, *trans*-cinnamic acid, *trans-m*-coumaric acid, *trans-p*-coumaric acid, triamcinolone, trigonelline hydrochloride, trioxsalen, ursolic acid, vina-ginsenoside R4, vincamine, wogonin, wogonoside, xanthotoxin, xylan from corn core, yohimbine hydrochloride, ι-carrageenan, κ-carrageenan, and λ-carrageenan (low-viscosity) were gained from TCI chemical (Tokyo, Japan). Formic acid was obtained from Fisher Scientific (Fair Lawn, NJ, USA). Sodium hydroxide, phosphoric acid, sulfuric acid, and ammonium acetate were purchased from Sigma Aldrich Co (St. Louis, MO, USA). Acetone, methanol, water, and acetonitrile (ACN) of HPLC grade were provided by J. T. Baker (Phillipsburg, NJ, USA). Ethyl alcohol (ethanol) and dichloro-

methane were provided by Daejung Chemicals & Metals Co. (Siheung-si, Kyunggido, South Korea). Dulbecco's Modified Eagle Medium (DMEM) with phenol red, fetal bovine serum (FBS), Dulbecco's phosphate-buffered saline (DPBS), and penicillin–streptomycin (P/S) were purchased from Biowest (Riverside, MO, USA).

Sample preparation

Standards of phytochemicals were dissolved in each suitable solvent. (−)-Cytisine, (+)-bicuculline, 3-(3,4-dihydroxyphenyl)-L-alanine, 4′,6,7-trihydroxyisoflavone, abietic acid, allantoin, andrographolide, baicalin, bergapten, bergenin, betulin, bisdemethoxycurcumin, cepharanthine, colchicine, cycloheximide, curcumin (natural), digoxin, ellagic acid, glycyrrhetic acid, harmine, hecogenin, icariin, LDN-22684, L-tetrahydropalmatine, lycorine, magnolol, matrine, mollugin, piperine, piperlongumine, parthenolide, phenethyl caffeate, piceid, rutaecarpine, resveratrol, rotenone, scopolamine hydrobromide trihydrate, sesamin, synephrine, tabersonine, tanshinone IIA, tetrahydropalmatine, tetrandrine, triamcinolone, vincamine, yohimbine hydrochloride, notoginsenoside R2, ginsenoside Rg5, and compound **K** were dissolved in dimethyl sulfoxide (DMSO), while (*S*)-(+)-camptothecin, oleuropein, paeoniflorin, wogonin, vina-ginsenoside R4, notoginsenoside R1, notoginsenoside Ft1, notoginsenoside Fe, gypenoside XLIX, gypenoside XVII, gypenoside L, ginsenoside Rh2, ginsenoside Rk3, ginsenoside Rh1, ginsenoside Rg4, ginsenoside Rg2, ginsenoside Rg1, ginsenoside Rf, ginsenoside Re, ginsenoside Rc, ginsenoside Rd, ginsenoside Rb3, ginsenoside Rb2, ginsenoside Rb1, ginsenoside F5, ginsenoside F4, ginsenoside F3, ginsenoside F2, ginsenoside F1, gramine, gypenoside A, 20(*S*)-ginsenoside Rg3, 20-*O*-glucoginsenoside Rf, 20(*R*)-ginsenoside Rh1, 20(*R*)-ginsenoside Rg2, and protopanaxatriol were dissolved in methanol. (−)-Dihydroquinine, (+)-nootkatone, (+)-taxifolin, (+)-usnic acid, (±)-evodiamine, 4′-hydroxy-3′-methoxyacetophenone, amygdalin, atropine, boldine, brucine hydrate, capsaicin (natural), cholecalciferol, curcumin (synthetic), ergosterol, gramicidin (mixture of **A**, **B**, **C** and **D**), griseofulvin, hematoxylin hydrate, hesperidin, hinokitiol, khellin, limonin, lanatoside C, nordihydroguaiaretic acid, noscapine hydrochloride hydrate, oridonine, papaverine hydrochloride, punicalagin, purpurin, quinidine, reserpine, santonin, sesamol, trioxsalen, ursolic acid, xanthotoxin, (*E*)-cinnamyl alcohol, aegeline, rosmarinic acid, *trans*-cinnamic acid, *trans-m*-coumaric acid, and *trans-p*-coumaric acid were dissolved in ethanol, and 2-(2-hydroxyethyl) phenol, 2-(4-hydroxyphenyl)ethanol, 3-methyl-1-phenyl-2-pyrazoline-5-one, 4-Formylphenyl β-D-allopyranoside, arbutin, bacitracin, berberine chloride hydrate, carminic acid (natural dye), cromolyn sodium salt, galantamine hydrobromide, glycyrrhizin, harmol, indican, jatrorrhizine chloride, mangiferin, phenazine methosulfate, pilocarpine hydrochloride, rhaponticin, rebaudioside A, rhododendrol, salicin, *S*-allyl-L-cysteine, sinigrin, swertiamarin, stevioside, trigonelline hydrochloride, wogonoside, xylan from corn core, ι-carrageenan, κ-carrageenan, λ-carrageenan (low-viscosity), (*E*)-3-(4-chlorophenyl)acrylic acid, and 3,5-dimethoxy-4-hydroxycinnamic acid were dissolved in water. Chrysazin was dissolved in acetone. Ellagic acid dihydrate in 1M Sodium hydroxide (NaOH) solution. Sclareol in dichloromethane.

HPLC-UV/ELSD analysis

To identify and quantify 162 phytochemicals, HPLC equipped with a photodiode array (PDA) detector (Nanospace SI-2, Osaka SODA Co., Ltd, Osaka, Japan) or Ultimate 3000 HPLC system with an UV-Vis detector (Thermo Fisher Scientific, Waltham, MA, USA) was utilized. Some samples were analyzed using Agilent 1200 series HPLC (Agilent Technologies, Santa Clara, CA, USA) - evaporative light scattering detection (ELSD) (ELSD-LT II, SHIMADAZU, Kyoto, Japan). The chromatographic columns used for the analysis of various phytochemicals are listed in Table S2. Each standard samples (20 mg) were dissolved in 2 mL of their respective solvent such as dimethyl sulfoxide (DMSO), methanol, ethanol, distilled water, acetone, 1M Sodium hydroxide solution, or dichloromethane. The mobile phase consisted of 0.05% (v/v) formic acid in distilled water (A) and 0.05% (v/v) formic acid in acetonitrile (B), with the elution gradient programmed as follows: 10 to 100% B over 35 min, followed by a return to 10% B within 5 min to regenerate the initial conditions. The flow rate was set at 0.7 mL min^{-1}, with an injection volume of 10 μL. The column temperature was maintained at 37 °C. For samples not suitable for this method, analysis was conducted using previously established or alternative methods. For the analysis of cromolyn sodium salt, the mobile phase consisted of 0.1% (v/v) sulfuric acid in distilled water (A) and 0.1% (v/v) sulfuric acid in acetonitrile (B), with the isocratic elution condition programmed as follows: 35% B over 15 min. The flow rate was set at 1.0 mL min^{-1}, with an injection volume of 10 μL. The column temperature was maintained at 37 °C. Analysis of ergosterol according to the previous method.[30] The mobile phase consisted of acetonitrile (B), and isocratic elution was performed at 100% B with a flow rate of 1.0 mL min^{-1} for 20 min. The injection volume was set to 10 μL, and the column temperature was maintained at 37 °C. For the analysis of cholecalciferol, the mobile phase consisted of distilled water (A) and acetonitrile (B), with the isocratic elution condition programmed as follows: 99% B over 25 min. The flow rate was ser at 1.0 mL min^{-1}, with an injection volume of 20 μL. The column temperature was maintained at 37 °C.[31] Analysis of ursolic acid according to the previous method.[32] The mobile phase consisted of distilled water (A) and methanol (B), and isocratic elusion was performed at 95% B with a flow rate of 0.4 mL min^{-1} for 25 min. The injection volume was set to 10 μL, and the column temperature was maintained at 37 °C. For the analysis of xylan from corn core, ι-carrageenan, κ-carrageenan, and λ-carrageenan (low-viscosity) using ELSD, mobile phase consisted of distilled water (A), and isocratic elusion was performed at 100% A with a flow rate of 0.8 mL min^{-1} for 30 min. The injection volume was set to 10 μL, and the column temperature was maintained at 37 °C.

In case of ginsenosides, as well as gypenoside A, gypenoside L, gypenoside XLIX, and gypenoside XVII, HPLC analysis was conducted using the Nanospace SI-2 system with a PDA detec-

tor. The mobile phase consisted of distilled water (A) and acetonitrile (B), with the gradient elution programmed as follows: 15% B at 0.5 min, increasing to 30% at 28.5 min, 32% at 30.5 min, 38% at 36.5 min, and 43% at 47.5 min. The proportion of B was further increased to 55% at 54.0 min and maintained at this level until 62.0 min. Subsequently, B increased to 70% at 70.0 min, followed by a further increase to 90% at 76.0 min and 95% at 76.1 min. This composition was held constant until 86.1 min, after which B rapidly decreased to 15% within 1 min to restore the initial conditions. The system was then equilibrated at 15% B until 93.0 min before the next injection. The flow rate, injection volume, and column temperature were maintained at 0.4 mL min^{-1}, 10 μL and 40 °C, respectively. Chromatograms for 162 phytochemicals were analyzed at various wavelengths, including 190, 194, 200, 203, 210, 230, 232, 235, 240, 250, 254, 268, 270, 275, 280, 282, 287, 290, 298, 300, 310, 320, 330, 360, 378, 380, and 420 nm, to maximize detection sensitivity.

Validation of an HPLC-UV/ELSD analytical method

The HPLC-UV analytical method for the quantification of 162 phytochemicals was validated in terms of linearity, accuracy, precision, and sensitivity, including the limits of detection (LOD) and quantification (LOQ). Linearity was assessed by analyzing three replicates at four concentration levels ranging from 1 to 50 μg mL^{-1}, 5 to 50 μg mL^{-1}, 10 to 100 μg mL^{-1}, or 50 to 500 μg mL^{-1}. The calibration curves were constructed, and the coefficient of determination (R^2) was calculated using the regression equation in Microsoft Excel 365. Accuracy was determined by evaluating the agreement between the measured and nominal concentrations, expressed as a percentage, calculated using the following equation:

$$\text{Accuracy } (\%) = \frac{\text{measured concentration}}{\text{nominal concentration}} \times 100$$

Precision was expressed as repeatability, representing the consistency of measurements obtained by the same analyst under identical conditions within a short time interval. Repeatability was evaluated by calculating the relative standard deviation (% RSD) using the equation:

$$\%\,\text{RSD} = \frac{\text{standard deviation of measured concentration}}{\text{mean of measured concentration}} \times 100$$

Sensitivity was determined based on LOD and LOQ, which were calculated from the calibration curve using the following equations:

$$\text{LOD} = 3.3 \times \frac{S_y}{S}$$

$$\text{LOQ} = 10 \times \frac{S_y}{S}$$

where S_y represents the standard deviation of the y-intercepts of the regression curves, and S denotes the slope of the calibration curve.

Culture of Caco-2 cell

Caco-2 human colon cancer cells were obtained from the Korean Cell Line Bank (KCLB, Seoul, Korea). The cells were cultured in Dulbecco's Modified Eagle Medium (DMEM) supplemented with 10% fetal bovine serum (FBS) and 1% penicillin–streptomycin (P/S) at 37 °C in a humidified atmosphere with 5% CO_2 and 95% air. The medium was replaced every 2 days, and sub-culturing was performed when cell confluence reached 70 to 80%. Cells were seeded in 12- well transwell culture plates (Corning, New York, USA) at a density of 1×10^5 cells per well and incubated at 37 °C in 5% CO_2, and the growth medium was refreshed every 2 days. All experiments were carried out with cells at passage numbers between 30 and 35. After being dissolved in their respective solvents, they were diluted to a final concentration of 100 μg mL^{-1} using DMEM prior to the permeability experiments. In order to compare permeability under identical mass loading rather than identical molar exposure across structurally diverse phytochemicals, consistent with a screening/formulation perspective, a uniform concentration of 100 μg mL^{-1} was applied to all compounds. As the apparent permeability coefficient (P_{app}) is normalized to the initial concentration, this approach allows comparative evaluation of structure–permeability relationships across diverse compound classes. The final concentrations of DMSO, methanol, and ethanol in the transport medium were maintained at 1% (v/v), and that of acetone was maintained at 0.5% (v/v), in order to minimize cytotoxic effects.[33–36] Studies have shown that a 1 M sodium hydroxide (NaOH) solution does not exert cytotoxic effects.[37] To evaluate that the solvents did not affect membrane integrity, TEER measurements were performed for all solvent conditions in the absence of phytochemicals.[38]

Bioavailability indicators through permeability experiments

Permeability experiments were initiated 21 days post-seeding to confirm the full differentiation of the Caco-2 monolayers, which were selected based on an initial transepithelial electrical resistance (TEER) value exceeding 300 Ω cm^{-2} to ensure the integrity of the epithelial cell barrier. TEER measurements were conducted using the Millicell ERS-2 system (Millipore, Bedford, MA, USA). To assess bi-directional permeability, a diluted standard solution of phytochemicals (100 μg mL^{-1}) was added to either the apical (AP, 500 μL) or basal (BL, 1500 μL) compartments. After a 2 hour incubation, 500 μL of the transport medium was collected from both sides, stored at 4 °C, and subsequently analyzed by high-performance liquid chromatography (HPLC). The 2 hour incubation time was selected based on previously established *in vitro* digestion models.[39–41] TEER values were recorded at 15, 45, 90, and 120 min, and the data were expressed as a percentage of the baseline (0 min) using the following equation:

$$\text{TEER } (\%\text{ of } 0 \text{ min}) = \frac{\text{TEER value at each time point}}{\text{TEER value at 0 min}} \times 100$$

The apparent permeability coefficients (P_{app}) and efflux ratio (ER) were calculated based on the following equations:

$$P_{app} = \frac{dQ}{dt} \times \frac{1}{C_0 \times A}$$

where (dQ/dt) represents the rate of phytochemical transport to the receiver side, expressed as the amount of substance transported per unit time after 120 min of incubation, C_0 is the initial concentration of phytochemicals in the donor compartment, and A is the membrane surface area (1.12 cm^2).

$$\text{Efflux ratio} = \frac{P_{app\,(BL\rightarrow AP)}}{P_{app\,(AP\rightarrow BL)}}$$

An efflux ratio greater than 2 suggests that the compounds may undergo active efflux. All bioavailability indicators of 162 phytochemicals were triplicated, consisting of 489 datasets.

The recovery of each compound, representing the remaining amount in both donor and receiver chambers at the end of the experiment, was calculated according to the following equation:

$$\%\,\text{recovery} = \frac{(C_r \cdot V_r + C_d \cdot V_d)}{(C_0 \cdot V_d)} \times 100$$

where C_r is the concentration in the receiver compartment at the end of the experiment, C_0 is the initial concentration in the donor compartment, C_d is the concentration in the donor compartment at the end of the experiment, and V_r and V_d are the volumes of the receiver and donor compartments, respectively.

Statistical analysis

All the data was determined by expressing as mean ± SD in triplicate. All statistical analyses were conducted in Python (version 3.11; Python Software Foundation). Non-parametric comparisons across chemical classes were performed using the Kruskal–Wallis test (SciPy; version 1.15.2), followed by Wilcoxon signed-rank tests against the theoretical baseline of 100% with Benjamini–Hochberg correction for false discovery rate (statsmodels; version 0.14.4). Data handling and summary statistics were carried out with pandas (version 2.2.3). Compound-level medians were calculated from three replicates per compound and reported as descriptive rankings without formal statistical inference due to limited replication. Although each compound was tested in triplicate, this replication number limits the statistical power. Future studies with larger replicate numbers and batch-to-batch validation are warranted to strengthen inference.

In addition to non-parametric tests, multivariate analysis was conducted to explore global relationships among permeability indices and physicochemical descriptors. Physicochemical parameters including topological polar surface area (TPSA, $Å^2$), number of hydrogen bond donors (HBD), number of hydrogen bond acceptors (HBA), and lipophilicity ($X\log P$) were retrieved from the PubChem database (National Center for Biotechnology Information, USA). These descriptors were automatically computed from canonical SMILES using the Cactvs toolkit (version 3.4.8) implemented in the PubChem Compound Summary service.

Principal component analysis (PCA) was performed using the scikit-learn package (version 1.6.1) in Python. Ten variables – recovery (AP → BL), AP → BL transport (%), BL → AP transport (%), $P_{app\ (AP\ \rightarrow\ BL)}$, $P_{app\ (BL\ \rightarrow\ AP)}$, efflux ratio, TPSA, HBD, HBA, and $X\log P$ – were standardized (z-scaling) prior to computation. The first two principal components (PC1 and PC2) were used for visualization, explaining the majority of variance across the dataset. PCA scores, loadings, and biplot figures were generated using Matplotlib (version 3.10.1) and Seaborn (version 0.13.2) to visualize multivariate associations among physicochemical descriptors and permeability-related parameters across structurally diverse phytochemicals.[42]

Pearson's correlation coefficients were computed using the SciPy package (version 1.15.2), and the resulting matrix was visualized as a heatmap using Seaborn (version 0.13.2) in Python.

Results and discussion

Bioanalytical method validation of various phytochemicals

The bioanalytical method for 162 phytochemicals, was validated by employing HPLC-UV or HPLC-ELSD in accordance with the bioanalytical method validation guidelines of the Ministry of Food and Drug Safety (MFDS), Republic of Korea.[43] Table S2 summarizes the validation results of 162 phytochemicals included parameters such as linearity, accuracy, precision, limit of detection (LOD), and limit of quantification (LOQ). Most of the phytochemicals exhibited good linearity, with correlation coefficients (R^2) exceeding 0.990 within the concentration range of 1–500 μg mL^{-1}, indicating a perfect linear fit. The accuracy values of the 162 phytochemicals ranged from 70.4% to 129.4%. Specifically, the accuracy values of alkaloids ranged from 70.4% to 127.2%, and those of amino acids ranged from 97.1% to 103.0%. For benzopyrans, the range was 96.0% to 120.3%, except for hematoxylin hydrate, which exhibited a broader range of 72.1% to 233.9%. Among cinnamic acids and derivatives, (*E*)-3-(4-chlorophenyl) acrylic acid showed accuracy values ranging from 76.7% to 187.3%, followed by 3,5-dimethoxy-4-hydroxycinnamic acid with values between 95.8% and 124.3%, while other compounds in this group exhibited narrower ranges between 94.0% and 103.7%. The accuracy values of flavonoids ranged from 93.4% to 109.9%, and those of ginsenosides were mostly between 90.6% and 106.4%, with a few exceptions displaying wider ranges. For glycosides, accuracy values were mostly between 90.0% and 116.5%. The ketones class showed accuracy values ranging from 89.2% to 101.7%. For phenolic compounds, most accuracy values ranged from 82.1% to 109.8%, although nordihydroguaiaretic acid exhibited a particularly wide range from 87.6% to 384.8%. Regarding polypeptides, the accuracy values ranged from 97.0% to 115.4%, while for polysaccharides, the range was between 94.3% and 104.8%. In the quinones class, carminic acid (a natural dye) exhibited the widest range of

accuracy values from 93.9% to 167.1%, whereas other quinone compounds ranged from 60.4% to 129.4%. The accuracy values for steroids ranged from 90.9% to 109.6%, and for terpenoids, they ranged from 92.2% to 106.8%, except for a few individual compounds with broader ranges. In the diazolidines, phenazines, and pyrazolones classes, each containing only one compound, the corresponding accuracy values ranged from 92.1% to 100.4%, 91.9% to 113.0%, and 95.0% to 100.9%, respectively. Results from the current study suggested that some of phytochemicals such as (*S*)-(+)-camptothecin and reserpine in alkaloids, (*E*)-3-(4-chlorophenyl) acrylic acid in cinnamic acid and its derivatives, salicin in glycosides, magnolol in phenolic compounds, and mollugin in quinones should need for further optimization in matrix-specific contexts.

The precision of the analytical method was evaluated by the percentage relative standard deviation (%RSD). Except for matrine, papaverine hydrochloride, (*E*)-3-(4-chlorophenyl) acrylic acid, carminic acid (natural dye), hecogenin, and sclareol, the precision values of the remaining analytes were generally below 20% (Table S1). The limits of detection (LOD) and quantification (LOQ) were determined, with results showing that the LOD ranged from 0.001 to 4.41 μg mL^{-1} and the LOQ ranged from 0.003 to 13.3 μg mL^{-1}. Overall, the developed bioanalytical method for 162 phytochemicals demonstrated robust, reproducible, and suitable for quantitative analysis of alkaloid compounds in complex matrices. Therefore, the developed bioanalytical method is suitable for the quantification of various phytochemicals in Caco-2 cell culture medium.

Effect of various phytochemicals on epithelial membrane in Caco-2 cell monolayer

The effects of 162 structurally diverse phytochemicals on epithelial barrier integrity were evaluated using TEER at 120 min and expressed as a percentage relative to baseline (0 min). As shown in Fig. S1, phytochemicals elicited heterogeneous barrier responses across chemical classes. Across all compounds, TEER values ranged from 44.4 ± 0.5% to 138.8 ± 10.2%, indicating both barrier-disruptive and barrier-enhancing effects depending on compound structure. Class-level differences in median TEER responses are summarized in Table 1 and visualized in Fig. S1. Nine chemical classes showed significant deviation from baseline ($q < 0.05$), with cinnamic acids and ketones enhancing barrier integrity, whereas alkaloids, terpenoids, and steroids tended to reduce it. Class-level TEER responses are summarized in Table 1, which presents median values normalized to baseline TEER (0 min = 100%) to facilitate comparison of barrier-modulating effects across phytochemical classes. As shown in Table 1, a global Kruskal–Wallis test confirmed significant differences among the 15 classes ($H = 74.31$, $p = 3.16 \times 10^{-10}$). Median % of TEER values indicated that several classes produced barrier-weakening effects, including polysaccharides (69.35%), diazolidines/phenazines/pyrazolones (75.00%), steroids (79.26%), terpenoids (86.48%), and alkaloids (89.18%). In contrast, barrier enhancement was observed in specific groups, notably cinnamic acids and derivatives showed 104.49% and ketones indicated 110.28%. Class-wise Wilcoxon signed-rank tests against the theoretical baseline of 100%, followed by Benjamini–Hochberg correction, revealed statistically significant decreases in alkaloids, terpenoids, glycosides, quinones, steroids, ginsenosides, polysaccharides, and diazolidines/phenazines/pyrazolones, whereas cinnamic acids and derivatives and ketones demonstrated significant increases ($q < 0.05$), implying that barrier-weakening effects predominate among several phytochemical classes, while only a limited subset (notably cinnamic acids and ketones) exert barrier-enhancing activity under the tested conditions.

At the individual compound level (median of three replicates), several phytochemicals emerged as barrier-strengthening candidates, including betulin (terpenoids, 138.65%),

Table 1 Class-level effects of phytochemical groups on % of TEER in Caco-2 monolayers

Class code	Chemical class	Median TEER%	*n* (wells)	Wilcoxon *p*-value	Adjusted *q*-value (BH)	Significant ($q < 0.05$)
A	Alkaloids	89.179	111	4.340×10^{-9}	6.511×10^{-8}	True
B	Amino acids	103.569	6	0.844	0.844	False
C	Benzopyrans	94.376	27	0.386	0.446	False
D	Cinnamic acids and derivatives	104.488	18	0.005	0.004	True
E	Flavonoids	97.696	21	0.452	0.485	False
F	Ginsenosides	95.876	90	0.020	0.034	True
G	Glycosides	94.311	57	9.656	0.0005	True
H	Ketones	110.281	6	0.031	0.047	True
I	Phenolic compounds	98.305	48	0.094	0.128	False
J	Polypeptides	90.346	6	0.219	0.273	False
K	Polysaccharides	69.354	12	0.016	0.030	True
L	Quinones	93.775	15	0.010	0.022	True
M	Steroids	79.263	9	0.004	0.010	True
N	Terpenoids	86.476	51	6.819	5.114×10^{-5}	True
O	Diazolidines/phenazines/pyrazolones	75.000	9	0.004	0.010	True

Median transepithelial electrical resistance (TEER) values of phytochemicals grouped by structural class after 120 min exposure in Caco-2 monolayers. TEER values are expressed as percentages relative to baseline (0 min = 100%). Median values represent class-level central tendencies across all tested compounds. Overall group differences were evaluated using the Kruskal–Wallis test (Wilcoxon *p*-value) with Benjamini–Hochberg (BH) correction for multiple comparisons (FDR $q < 0.05$). *n* (wells) indicates the total number of replicate wells included for all compounds within each structural class, with each individual compound measured in triplicate.

icariin (flavonoids, 128.24%), ι-carrageenan (polysaccharides, 125.39%), 20-*O*-glucoginsenoside Rf (ginsenosides, 121.89%), and compound **K** (ginsenosides, 121.89%). Conversely, pronounced barrier disruption was associated with Hecogenin (terpenoids, 44.41%), ergosterol (steroids, 46.39%), sclareol (terpenoids, 46.48%), capsaicin (alkaloids, 49.51%), and carminic acid (quinones, 55.98%).

The barrier-enhancing effects observed for cinnamic acids and ketones may be associated with the up-regulation or stabilization of tight-junction proteins (*e.g.*, ZO-1 and occludin), a mechanism widely reported for dietary polyphenols and nutrient factors that preserve epithelial integrity.[44,45] Conversely, certain phytochemical classes that reduced TEER in this study, such as alkaloids, may modulate paracellular permeability through transient alterations in junctional complexes and cytoskeletal organization, as reported for capsaicin in Caco-2 monolayers.[46,47] The effects of terpenoids on epithelial barrier function appear to be structure- and context-dependent, requiring further investigation to clarify their impact under physiological and stress conditions.

Collectively, these observations indicate class-dependent alterations in epithelial barrier integrity, consistent with the heterogeneous chemical structures of the tested phytochemicals. Compounds with higher polarity tended to maintain TEER, whereas moderately lipophilic structures such as certain flavonoids or benzopyrans caused transient decreases without barrier disruption, supporting that polarity and lipophilicity govern epithelial permeability by modulating tight-junction dynamics rather than inducing cytotoxic damage.[44,48,49]

To our knowledge, this study represents the first systematic statistical evaluation of epithelial barrier integrity based on TEER measurements across diverse phytochemical groups. Given that each compound was assessed in only three replicates, compound-level statistical comparisons did not survive false discovery rate adjustment. Accordingly, the observed rankings should be regarded as preliminary, effect-size–driven screening results that require confirmation in future studies with larger sample sizes and more rigorously controlled conditions, including batch and vehicle normalization.

Transport of various phytochemicals across intestinal monolayer

Table 2 summarizes Caco-2 transport outcomes for the compound set, including recovery (AP → BL), transported fraction (AP → BL and BL → AP), bidirectional apparent permeability (P_{app}; $\times 10^{-6}$ cm s^{-1}), and efflux ratio ($P_{app\ (BL\rightarrow AP)}/P_{app\ (AP\rightarrow BL)}$). Because some entries were reported as N/A or N/D, the number of evaluable data points varied by endpoint. Recovery (AP → BL) was available for 87 compounds (median 93.7%, range 19.6–124.1%). The transported fraction was reported for 101 compounds for AP → BL (median 10.8%, range 0.18–118.9%) and 111 compounds for BL → AP (median 4.41%, range 0.013–102.1%). P_{app} values were available for 101 compounds in the AP → BL direction (median 10.1, range 0.11–129.0 $\times 10^{-6}$ cm s^{-1}) and 111 compounds in the BL → AP direction (median 6.01, range 0.05–59.3 $\times 10^{-6}$ cm s^{-1}). The efflux ratio was calculable for 100 compounds, with a median of 0.735 and a wide range (0.005–22.2). The highest AP → BL permeability was observed for bergapten (129.0 $\times 10^{-6}$ cm s^{-1}), while the lowest AP → BL permeability and the largest directional asymmetry were observed for cromolyn sodium salt ($P_{app\ (AP\rightarrow BL)}$ 0.11, efflux ratio 22.2). Overall, Table 2 indicates substantial inter-compound variability in permeability and clear directional asymmetry in a subset of compounds. Cases where BL → AP transport exceeded AP → BL (*i.e.*, higher efflux ratios) are consistent with the possibility of carrier-mediated efflux and/or polarized transport processes, whereas the opposite asymmetry may reflect preferential absorptive transport, differential membrane interactions, or experimental matrix effects. These observations motivate interpreting permeability together with bidirectional P_{app} patterns rather than relying on a single threshold-based classification.

Previous study found that recovery values are critical for interpreting permeability data in Caco-2 monolayers and the low recovery rates observed for compounds may be attributed to poor solubility, adsorption to the plate, intracellular accumulation, or metabolic transformation within the Caco-2 cells.[50,51] Recovery variability observed in this study is consistent with the diverse physicochemical properties of phytochemicals and with previous reports indicating that incomplete recovery in Caco-2 assays may arise from limited solubility, adsorption to experimental surfaces, intracellular accumulation, or metabolic transformation during incubation.[29,52] Given the substantial structural diversity and varying physicochemical properties of the tested compounds, the following analysis is presented primarily as a descriptive comparison of permeability-related behavior rather than as a definitive quantitative ranking across all phytochemicals.

Table 2 also presents the apparent permeability coefficients (P_{app}) of the 162 phytochemicals, which represent the rate of transport across Caco-2 monolayers. Previous studies have suggested empirical relationships between P_{app} values and *in vivo* absorption potential, where values $\leq 1 \times 10^{-6}$ cm s^{-1} are generally associated with low permeability, values between 1×10^{-6} and 10×10^{-6} cm s^{-1} with moderate permeability, and values $>10 \times 10^{-6}$ cm s^{-1} with relatively high permeability.[53] Comparison with commonly referenced permeability thresholds indicates that many alkaloids and certain aglycones fall within the high-permeability range ($>10 \times 10^{-6}$ cm s^{-1}), consistent with previously reported Caco-2–based permeability classifications and historical correlations between Caco-2 transport and human intestinal absorption.[29,53] These thresholds should be interpreted as comparative *in vitro* indicators rather than direct predictors of *in vivo* absorption. In contrast, ginsenosides, polypeptides, and polysaccharides remained largely undetectable under the present experimental conditions, in line with previous reports indicating that glycosylation and larger molecular size have been reported to limit epithelial permeability.[54–56] Quinidine, a *P*-glycoprotein substrate, exhibited ER > 2 as expected.[57] Piperine also showed ER > 2; however, literature suggests it often acts as a *P*-gp modulator and has been reported to increase the bioavailability of

Table 2 Recovery, apparent permeability coefficients (P_{app}), and efflux ratios (ER) of representative phytochemicals measured in Caco-2 monolayers

Compound	Recovery (AP → BL) (%)	AP to BL (%)	BL to AP (%)	P_{app} ($\times 10^{-6}$ cm s^{-1})		Efflux ratio ($P_{app\ (BL\rightarrow AP)}$/ $P_{app\ (AP\rightarrow BL)}$)
				$P_{app\ (AP\rightarrow BL)}$	$P_{app\ (BL\rightarrow AP)}$	
Alkaloids						
(−)-Cytisine	101.7 ± 0.4	13.0 ± 0.1	2.25 ± 0.03	8.09 ± 0.09	4.19 ± 0.06	0.52 ± 0.001
(−)-Dihydroquinine	74.3 ± 1.1	16.3 ± 0.3	5.98 ± 0.6	10.1 ± 0.4	11.1 ± 0.8	1.10 ± 0.1
(+)-Bicuculline	n.d.	N/D	N/D	N/A	N/A	N/A
(±)-Evodiamine	n.d.	6.97 ± 0.01	N/D	8.8 ± 0.02	N/A	N/A
(*S*)-(+)-Camptothecin	n.d.	N/D	N/D	N/A	N/A	N/A
Aegeline	n.d.	0.73 ± 0.1	0.60 ± 0.03	0.92 ± 0.15	0.24 ± 0.01	0.27 ± 0.05
Atropine	n.d.	15.1 ± 0.8	6.46 ± 0.03	18.5 ± 1.03	7.94 ± 0.1	0.43 ± 0.02
Berberine chloride Hydrate	n.d.	3.56 ± 0.03	12.1 ± 0.005	4.15 ± 0.03	14.09 ± 0.005	3.39 ± 0.03
Boldine	82.6 ± 0.3	16.0 ± 0.7	6.24 ± 0.007	9.89 ± 0.4	11.6 ± 0.01	1.17 ± 0.05
Brucine hydrate	n.d.	54.3 ± 0.6	27.6 ± 0.3	68.5 ± 0.8	10.7 ± 0.1	0.16 ± 0.0001
Capsaicin (natural)	n.d.	37.2 ± 1.08	44.0 ± 0.9	10.0 ± 0.3	11.8 ± 0.2	1.18 ± 0.06
Cepharanthine	42.4 ± 1.7	1.22 ± 0.3	0.25 ± 0.09	0.75 ± 0.2	0.46 ± 0.2	0.61 ± 0.2
Colchicine	93.06 ± 1.2	4.09 ± 0.08	4.44 ± 2.1	2.54 ± 0.05	8.28 ± 4.02	3.28 ± 1.6
Galantamine Hydrobromide	102.3 ± 3.6	30.8 ± 1.8	8.67 ± 0.2	19.1 ± 1.1	16.1 ± 0.5	0.85 ± 0.04
Gramine	n.d.	72.5 ± 1.53	46.0 ± 0.07	91.5 ± 1.9	18.2 ± 0.03	0.20 ± 0.004
Harmine	n.d.	15.1 ± 6.24	13.7 ± 0.15	19.0 ± 0.08	5.42 ± 0.06	0.28 ± 0.002
Harmol	37.8 ± 5.03	6.54 ± 0.2	2.27 ± 0.04	4.06 ± 0.10	4.22 ± 0.07	1.04 ± 0.008
Jatrorrhizine chloride	94.6 ± 8.4	1.95 ± 1.4	0.66 ± 0.04	1.21 ± 0.9	1.22 ± 0.08	1.64 ± 1.4
L-Tetrahydropalmatine	86.1 ± 3.2	23.0 ± 2.7	9.61 ± 2.0	14.3 ± 1.7	17.9 ± 3.7	1.25 ± 0.1
Lycorine	89.2 ± 1.4	22.0 ± 0.9	5.74 ± 0.2	13.6 ± 0.5	13.2 ± 0.5	0.97 ± 0.07
Matrine	n.d.	N/D	N/D	N/A	N/A	N/A
Noscapine Hydrochloride hydrate	n.d.	0.86 ± 0.009	7.24 ± 0.9	1.06 ± 0.01	8.89 ± 1.1	8.38 ± 1.002
Papaverine hydrochloride	n.d.	13.6 ± 0.8	2.76 ± 8.7	17.1 ± 1.0	1.1 ± 0.03	0.06 ± 0.002
Pilocarpine hydrochloride	n.d.	N/D	N/D	N/A	N/A	N/A
Piperine	105.9 ± 8.5	29.1 ± 2.6	19.4 ± 0.2	18.02 ± 1.6	36.2 ± 0.3	2.02 ± 0.2
Piperlongumine	77.7 ± 6.6	18.05 ± 0.3	6.36 ± 0.7	11.2 ± 0.2	11.8 ± 1.3	1.06 ± 0.1
Quinidine	n.d.	12.8 ± 0.5	25.4 ± 1.6	16.2 ± 0.6	59.3 ± 43.3	3.66 ± 2.7
Reserpine	26.4 ± 2.008	N/D	10.5 ± 0.9	N/A	19.5 ± 1.6	N/A
Rutaecarpine	31.5 ± 1.2	N/D	2.59 ± 0.09	N/A	4.82 ± 0.2	N/A
Scopolamine hydrobromide trihydrate	73.1 ± 3.9	19.5 ± 4.4	7.64 ± 0.4	12.1 ± 2.7	14.2 ± 0.8	1.22 ± 0.3
Synephrine	n.d.	N/D	N/D	N/A	N/A	N/A
Tabersonine	124.1 ± 22.3	N/D	1.15 ± 0.06	N/A	2.15 ± 0.1	N/A
Tetrahydropalmatine	87.8 ± 1.3	16.7 ± 0.3	6.31 ± 0.03	10.4 ± 0.2	11.7 ± 0.05	1.13 ± 0.02
Tetrandrine	48.1 ± 2.3	10.8 ± 1.16	1.02 ± 0.04	6.67 ± 0.7	1.90 ± 0.07	0.29 ± 0.04
Trigonelline Hydrochloride	104.1 ± 2.89	N/D	N/D	N/A	N/A	N/A
Vincamine	103.02 ± 4.4	19.7 ± 1.3	6.39 ± 1.5	12.2 ± 0.8	11.9 ± 2.7	0.96 ± 0.15
Yohimbine Hydrochloride	87.9 ± 2.5	19.4 ± 2.8	3.99 ± 0.3	12.0 ± 1.7	7.42 ± 0.6	0.63 ± 0.1
Amino acids						
3-(3,4-Dihydroxyphenyl)-L-alanine	n.d.	6.09 ± 0.9	16.5 ± 1.6	7.49 ± 1.1	20.3 ± 2.0	2.76 ± 0.6
S-allyl-L-cysteine	n.d.	N/D	N/D	N/A	N/A	N/A
Benzopyrans						
Bergapten	n.d.	118.9 ± 4.9	102.1 ± 5.2	129.0 ± 6.58	47.2 ± 1.93	0.37 ± 0.02
Bergenin	n.d.	15.2 ± 0.3	8.49 ± 0.05	19.2 ± 0.4	10.7 ± 0.06	0.56 ± 0.008
Cromolyn sodium salt	93.7 ± 0.004	0.18 ± 0.2	0.53 ± 0.2	0.11 ± 0.13	0.77 ± 0.3	22.2 ± 27.6
Griseofulvin	n.d.	17.4 ± 0.3	8.3 ± 0.6	10.5 ± 0.8	6.92 ± 0.1	0.66 ± 0.05
Hematoxylin hydrate	n.d.	0.25 ± 0.06	1.16 ± 0.3	0.30 ± 0.08	1.44 ± 0.3	5.1 ± 2.2
Khellin	n.d.	20.6 ± 0.8	24.8 ± 0.6	26.0 ± 1.0	9.86 ± 0.3	0.4 ± 0.01
Mangiferin	111.0 ± 3.2	8.72 ± 2.6	2.00 ± 0.1	5.41 ± 1.6	3.71 ± 0.2	0.74 ± 0.2
Trioxsalen	19.6 ± 1.3	15.4 ± 1.1	9.47 ± 1.2	9.57 ± 0.7	17.6 ± 2.1	1.84 ± 0.1
Xanthotoxin	91.2 ± 5.0	28.8 ± 1.4	10.1 ± 0.5	17.9 ± 0.9	18.9 ± 1.0	1.06 ± 0.1
Cinnamic acids and derivatives						
(*E*)-3-(4-Chlorophenyl)acrylic Acid	n.d.	23.0 ± 4.7	15.9 ± 0.4	20.1 ± 0.5	9.13 ± 1.9	0.45 ± 0.09
(*E*)-Cinnamyl Alcohol	n.d.	3.49 ± 0.3	1.22 ± 0.06	4.41 ± 0.4	1.54 ± 0.08	0.35 ± 0.04
3,5-Dimethoxy-4-hydroxycinnamic acid	n.d.	5.85 ± 0.3	5.08 ± 0.2	7.39 ± 0.4	2.02 ± 0.06	0.27 ± 0.02
trans-Cinnamic acid	n.d.	48.7 ± 22.9	18.2 ± 8.6	11.7 ± 1.6	10.0 ± 1.1	0.86 ± 0.1
trans-m-Coumaric acid	n.d.	10.1 ± 0.5	0.54 ± 0.0002	12.5 ± 0.7	0.21 ± 0.00009	0.02 ± 0.0009
trans-p-Coumaric acid	n.d.	9.25 ± 0.06	0.13 ± 0.003	11.4 ± 0.08	0.05 ± 0.001	0.005 ± 0.0001
Flavonoids						
(+)-Taxifolin	72.2 ± 2.2	5.90 ± 0.9	2.93 ± 1.4	3.66 ± 0.5	5.44 ± 2.6	1.59 ± 1.0
4′,6,7-Trihydroxyisoflavone	84.3 ± 2.8	1.43 ± 0.7	3.75 ± 1.3	0.89 ± 0.5	6.97 ± 2.4	11.7 ± 11.3
Icariin	78.7 ± 0.4	0.32 ± 0.02	1.37 ± 0.08	0.20 ± 0.01	2.54 ± 0.1	12.8 ± 1.7
Phenethyl caffeate	49.5 ± 1.2	2.56 ± 0.2	3.00 ± 0.1	1.59 ± 0.1	5.57 ± 0.3	3.52 ± 0.06
Rotenone	n.d.	5.36 ± 3.5	1.47 ± 0.6	6.59 ± 4.3	1.81 ± 0.7	0.61 ± 0.8
Wogonin	68.9 ± 0.4	42.6 ± 0.2	9.16 ± 0.2	26.4 ± 0.1	17.04 ± 0.3	0.65 ± 0.01
Wogonoside	96.8 ± 1.7	2.36 ± 1.4	1.32 ± 0.2	1.46 ± 0.9	2.46 ± 0.4	1.98 ± 0.8

Table 2 *(Contd.)*

Compound	Recovery (AP → BL) (%)	AP to BL (%)	BL to AP (%)	P_{app} ($\times 10^{-6}$ cm s^{-1})		Efflux ratio ($P_{app\ (BL\rightarrow AP)}$/ $P_{app\ (AP\rightarrow BL)}$)
				$P_{app\ (AP\rightarrow BL)}$	$P_{app\ (BL\rightarrow AP)}$	
Ginsenoside						
20(R)-Ginsenoside Rg2	96.6 ± 0.8	N/D	N/D	N/A	N/A	N/A
20(R)-Ginsenoside Rh1	92.1 ± 1.0	N/D	N/D	N/A	N/A	N/A
20(S)-Ginsenoside Rg3	95.6 ± 4.3	N/D	N/D	N/A	N/A	N/A
20-O-Glucoginsenoside Rf	98.006 ± 1.1	N/D	N/D	N/A	N/A	N/A
Compound **K**	90.1 ± 0.9	N/D	N/D	N/A	N/A	N/A
Ginsenoside F1	95.04 ± 0.3	N/D	2.45 ± 0.03	N/A	4.56 ± 0.06	N/A
Ginsenoside F2	94.9 ± 2.7	N/D	N/D	N/A	N/A	N/A
Ginsenoside F3	96.9 ± 2.0	N/D	N/D	N/A	N/A	N/A
Ginsenoside F4	99.2 ± 1.1	N/D	N/D	N/A	N/A	N/A
Ginsenoside F5	98.5 ± 0.6	N/D	3.81 ± 0.1	N/A	7.09 ± 0.3	N/A
Ginsenoside Rb1	99.6 ± 0.2	N/D	N/D	N/A	N/A	N/A
Ginsenoside Rb2	99.2 ± 0.02	N/D	3.21 ± 0.03	N/A	5.96 ± 0.05	N/A
Ginsenoside Rb3	96.1 ± 0.2	N/D	N/D	N/A	N/A	N/A
Ginsenoside Rc	117.5 ± 2.01	20.2 ± 0.4	2.24 ± 0.2	12.5 ± 0.3	4.16 ± 0.3	0.33 ± 0.03
Ginsenoside Rd	104.01 ± 0.2	N/D	N/D	N/A	N/A	N/A
Ginsenoside Re	100.04 ± 1.3	N/D	N/D	N/A	N/A	N/A
Ginsenoside Rf	97.4 ± 0.2	N/D	0.79 ± 0.02	N/A	1.46 ± 0.04	N/A
Ginsenoside Rg1	95.4 ± 2.1	N/D	N/D	N/A	N/A	N/A
Ginsenoside Rg2	98.7 ± 0.4	N/D	N/D	N/A	N/A	N/A
Ginsenoside Rg4	104.5 ± 1.1	N/D	N/D	N/A	N/A	N/A
Ginsenoside Rg5	72.6 ± 1.9	N/D	N/D	N/A	N/A	N/A
Ginsenoside Rh1	98.5 ± 1.0	2.48 ± 0.2	0.48 ± 0.1	1.54 ± 0.1	0.9 ± 0.2	0.58 ± 0.1
Ginsenoside Rh2	83.4 ± 3.4	N/D	N/D	N/A	N/A	N/A
Ginsenoside Rk3	92.003 ± 2.3	N/D	0.18 ± 0.03	N/A	0.33 ± 0.06	N/A
Notoginsenoside Fe	96.9 ± 2.4	N/D	N/D	N/A	N/A	N/A
Notoginsenoside Ft1	87.3 ± 0.9	N/D	N/D	N/A	N/A	N/A
Notoginsenoside R1	96.7 ± 1.8	N/D	N/D	N/A	N/A	N/A
Notoginsenoside R2	100.4 ± 1.6	N/D	N/D	N/A	N/A	N/A
Protopanaxatriol	76.9 ± 6.7	12.1 ± 0.1	3.23 ± 0.05	7.50 ± 0.07	6.01 ± 0.09	0.81 ± 0.0008
Vina-ginsenoside R4	101.1 ± 1.7	N/D	N/D	N/A	N/A	N/A
Glycosides						
Gypenoside A	95.2 ± 0.4	N/D	N/D	N/A	N/A	N/A
Gypenoside L	89.5 ± 4.0	N/D	N/D	N/A	N/A	N/A
Gypenoside XLIX	95.0 ± 2.2	N/D	N/D	N/A	N/A	N/A
Gypenoside XVII	94.8 ± 0.6	N/D	N/D	N/A	N/A	N/A
4-Formylphenyl β-D-allopyranoside	n.d.	12.4 ± 0.3	4.21 ± 0.2	15.3 ± 0.4	5.18 ± 0.3	0.34 ± 0.02
Amygdalin	n.d.	66.7 ± 10.9	30.01 ± 3.6	82.0 ± 13.3	36.9 ± 4.43	0.46 ± 0.09
Arbutin	n.d.	11.1 ± 0.3	21.7 ± 1.4	13.6 ± 0.3	26.7 ± 1.7	1.96 ± 0.08
Baicalin	n.d.	1.76 ± 0.1	0.44 ± 0.01	1.81 ± 0.1	0.45 ± 0.01	0.25 ± 0.02
Digoxin	82.8 ± 0.4	N/D	1.82 ± 0.2	N/A	3.38 ± 0.3	N/A
Hesperidin	n.d.	1.05 ± 0.01	0.30 ± 0.004	1.29 ± 0.01	0.37 ± 0.005	0.29 ± 0.006
Indican	90.7 ± 7.3	5.96 ± 2.6	0.75 ± 0.05	3.69 ± 1.6	1.40 ± 0.09	0.42 ± 0.1
Lanatoside C	89.5 ± 0.2	N/D	N/D	N/A	N/A	N/A
Piceid	n.d.	0.92 ± 0.1	6.65 ± 2.1	1.13 ± 0.2	2.64 ± 0.8	2.35 ± 0.7
Rebaudioside A	n.d.	1.24 ± 0.01	1.96 ± 0.05	1.52 ± 0.002	2.40 ± 0.07	1.58 ± 0.04
Rhaponticin	101.7 ± 3.8	49.5 ± 0.4	5.79 ± 0.1	30.7 ± 0.3	10.8 ± 0.1	0.35 ± 0.001
Salicin	n.d.	38.8 ± 13.6	12.3 ± 6.0	47.7 ± 16.7	19.9 ± 9.84	0.41 ± 0.09
Sinigrin	78.01 ± 14.2	16.3 ± 9.1	4.09 ± 2.3	10.1 ± 5.62	7.61 ± 4.20	1.42 ± 1.2
Stevioside	n.d.	0.80 ± 0.2	1.01 ± 0.2	1.00 ± 0.2	1.24 ± 0.3	1.34 ± 0.5
Swertiamarin	95.4 ± 1.5	2.64 ± 0.4	0.46 ± 0.1	1.64 ± 0.2	0.85 ± 0.1	0.52 ± 0.01
Ketones						
4′-Hydroxy-3′-methoxyacetophenone	n.d.	16.1 ± 0.3	18.8 ± 0.5	20.3 ± 0.4	22.6 ± 0.6	1.11 ± 0.04
Cycloheximide	37.6 ± 21.7	N/D	4.71 ± 0.8	N/A	8.76 ± 1.5	N/A
Phenolic compounds						
(+)-Usnic acid	n.d.	2.73 ± 0.5	2.99 ± 0.04	3.44 ± 0.6	1.19 ± 0.02	0.35 ± 0.1
2-(2-Hydroxyethyl)phenol	n.d.	13.0 ± 0.2	28.9 ± 0.4	15.9 ± 0.2	35.5 ± 0.5	2.23 ± 0.02
2-(4-Hydroxyphenyl)ethanol	n.d.	11.8 ± 0.3	23.1 ± 0.2	14.5 ± 0.3	28.4 ± 0.2	1.96 ± 0.04
Bisdemethoxycurcumin	n.d.	2.91 ± 0.3	0.94 ± 0.04	3.67 ± 0.3	1.18 ± 0.06	0.32 ± 0.04
Curcumin (natural)	n.d.	14.8 ± 0.3	1.10 ± 0.5	18.2 ± 0.3	1.35 ± 0.6	0.07 ± 0.04
Curcumin (synthetic)	n.d.	N/D	N/D	N/A	N/A	N/A
Ellagic acid	n.d.	N/D	N/D	N/A	N/A	N/A
Ellagic acid Dihydrate	n.d.	53.9 ± 1.9	5.76 ± 0.6	66.1 ± 3.11	7.06 ± 0.4	0.11 ± 0.01
Magnolol	n.d.	6.90 ± 0.03	1.40 ± 0.005	8.48 ± 0.04	1.72 ± 0.006	0.20 ± 0.0002
Nordihydroguaiaretic acid	n.d.	N/D	N/D	N/A	N/A	N/A
Punicalagin	n.d.	7.39 ± 0.5	4.41 ± 3.2	9.09 ± 0.6	5.42 ± 3.9	0.59 ± 0.4
Resveratrol	n.d.	N/D	17.3 ± 1.2	N/A	21.3 ± 1.5	N/A
Rhododendrol	n.d.	10.7 ± 1.4	31.8 ± 0.5	13.5 ± 1.8	12.6 ± 0.2	0.95 ± 0.1

Table 2 *(Contd.)*

Compound	Recovery (AP → BL) (%)	AP to BL (%)	BL to AP (%)	P_{app} ($\times 10^{-6}$ cm s^{-1})		Efflux ratio ($P_{app\ (BL\rightarrow AP)}/P_{app\ (AP\rightarrow BL)}$)
				$P_{app\ (AP\rightarrow BL)}$	$P_{app\ (BL\rightarrow AP)}$	
Rosmarinic acid	n.d.	44.7 ± 0.4	13.7 ± 0.4	56.5 ± 0.5	5.44 ± 0.2	0.096 ± 0.003
Sesamin	n.d.	N/D	N/D	N/A	N/A	N/A
Sesamol	n.d.	5.36 ± 3.9	1.45 ± 1.5	6.59 ± 4.81	1.78 ± 1.8	0.28 ± 0.1
Polypeptides						
Bacitracin	96.2 ± 2.8	3.53 ± 0.5	0.478 ± 0.02	2.19 ± 0.3	0.89 ± 0.04	0.41 ± 0.04
Gramicidin (mixture of A, B, C, and D)	93.6 ± 11.0	N/D	N/D	N/A	N/A	N/A
Polysaccharides						
Xylan from corn core	n.d.	N/D	N/D	N/A	N/A	N/A
ι-Carrageenan	n.d.	N/D	N/D	N/A	N/A	N/A
κ-Carrageenan	n.d.	N/D	N/D	N/A	N/A	N/A
λ-Carrageenan (low-viscosity)	n.d.	N/D	N/D	N/A	N/A	N/A
Quinones						
Carminic acid (natural dye)	94.2 ± 1.1	1.83 ± 0.9	0.43 ± 0.4	1.14 ± 0.5	0.80 ± 0.8	0.78 ± 0.8
Chrysazin	n.d.	8.11 ± 1.6	20.1 ± 1.7	10.2 ± 2.0	7.98 ± 0.7	0.80 ± 0.2
LDN-22684	110.2 ± 2.1	22.4 ± 0.9	5.23 ± 0.1	13.9 ± 0.5	9.73 ± 0.1	0.70 ± 0.02
Mollugin	n.d.	N/D	N/D	N/A	N/A	N/A
Purpurin	n.d.	N/D	N/D	N/A	N/A	N/A
Steroids						
Cholecalciferol	100.2 ± 8.1	2.31 ± 0.7	0.013 ± 0.02	1.43 ± 0.4	0.11 ± 0.1	0.06 ± 0.07
Ergosterol	100.6 ± 3.8	21.2 ± 6.7	1.40 ± 0.3	10.6 ± 5.3	2.60 ± 0.6	0.27 ± 0.07
Triamcinolone	95.5 ± 1.1	4.25 ± 0.24	3.47 ± 0.18	2.63 ± 0.1	6.46 ± 0.3	2.45 ± 0.03
Terpenoids						
(+)-Nootkatone	77.8 ± 3.1	16.4 ± 0.5	9.65 ± 0.3	10.2 ± 0.3	17.9 ± 0.5	1.77 ± 0.1
Abietic acid	n.d.	9.90 ± 3.6	6.61 ± 0.3	12.5 ± 4.5	8.35 ± 0.4	0.73 ± 0.3
Andrographolide	n.d.	8.85 ± 0.5	7.82 ± 0.2	11.2 ± 0.6	9.88 ± 0.3	0.89 ± 0.1
Betulin	n.d.	26.8 ± 4.3	15.03 ± 6.8	33.0 ± 5.2	18.5 ± 8.35	0.55 ± 0.2
Glycyrrhetic acid	n.d.	5.55 ± 0.2	8.45 ± 0.3	6.82 ± 0.2	3.35 ± 0.1	0.49 ± 0.0003
Glycyrrhizin	n.d.	11.0 ± 0.2	2.34 ± 0.03	13.5 ± 0.2	1.22 ± 0.02	0.09 ± 0.0004
Hecogenin	n.d.	8.33 ± 1.3	4.60 ± 2.3	10.2 ± 1.6	5.71 ± 2.8	0.59 ± 0.37
Hinokitiol	n.d.	9.86 ± 0.3	16.6 ± 0.7	12.1 ± 0.4	20.0 ± 0.8	1.65 ± 0.1
Limonin	n.d.	N/D	N/D	N/A	N/A	N/A
Oleuropein	82.8 ± 0.5	2.67 ± 0.1	1.09 ± 0.2	1.65 ± 0.05	2.03 ± 0.4	1.22 ± 0.2
Oridonine	81.2 ± 1.7	4.01 ± 0.05	2.02 ± 0.1	2.48 ± 0.03	3.76 ± 0.2	1.51 ± 0.1
Paeoniflorin	20.8 ± 0.8	14.6 ± 0.7	1.38 ± 0.1	9.07 ± 0.4	2.56 ± 0.1	0.28 ± 0.01
Parthenolide	n.d.	N/D	N/D	N/A	N/A	N/A
Santonin	92.2 ± 0.7	19.7 ± 0.3	13.5 ± 0.2	12.2 ± 0.2	25.1 ± 0.3	2.05 ± 0.02
Sclareol	n.d.	N/D	N/D	N/A	N/A	N/A
Tanshinone IIA	87.0 ± 5.6	N/D	N/D	N/A	N/A	N/A
Ursolic acid	n.d.	N/D	N/D	N/A	N/A	N/A
Diazolidines						
Allantoin	n.d.	66.7 ± 10.9	30.0 ± 3.6	82.0 ± 13.3	36.9 ± 4.4	0.46 ± 0.09
Phenazines						
Phenazine methosulfate	49.1 ± 0.8	8.21 ± 0.6	4.37 ± 0.03	5.09 ± 0.4	8.12 ± 0.06	1.60 ± 0.1
Pyrazolones						
3-Methyl-1-phenyl-2-pyrazoline-5-one	50.2 ± 0.1	0.78 ± 0.2	2.94 ± 0.1	0.49 ± 0.09	5.48 ± 0.2	11.6 ± 2.6

Recovery values are expressed as percentages of the initial concentration. Apparent permeability coefficients (P_{app}) are reported for both apical-to-basolateral (AP → BL) and basolateral-to-apical (BL → AP) transport directions. Efflux ratios were calculated as $P_{app\ (BL\rightarrow AP)}/P_{app\ (AP\rightarrow BL)}$. Values are presented as mean ± SD. n.d., not determined due to lack of baseline apical concentration data; N/D, not detected (quantitative amount below the limit of detection); N/A, not available due to insufficient data for calculation.

co-administered drugs *via* efflux inhibition.[58,59] This apparent discrepancy highlights the need for transporter-specific inhibitor studies to clarify whether piperine primarily functions as a substrate, inhibitor, or context-dependent modulator. Besides *P*-glycoprotein, other efflux transporters such as BCRP and MRP2 may also contribute to the observed efflux-prone behavior, as suggested by previous studies.[60] Future transporter-specific inhibition or gene-silencing assays are warranted to confirm these mechanisms. Overall, compounds with lower molecular weight (<400 Da) and moderate lipophilicity ($\log P \approx$ 1–4) – such as piperine, quinidine, wogonin, and ursolic acid – tended to exhibit higher P_{app} and moderate TEER reduction, indicating favorable transcellular diffusion.[48,49,61] In contrast, highly polar or glycosidic molecules, including rutin, ginsenoside Rb1, and amygdalin, showed markedly reduced P_{app} and stable TEER, consistent with their hydrophilicity and large polar surface areas.[62,63] Together, these results suggest that the intestinal absorption potential of phytochemicals may be broadly associated with their physicochemical characteristics, supporting the structure–permeability relationships reflected in the present dataset.

Although the present study focused primarily on the establishment of a high-quality experimental dataset, the accumulated data may be further leveraged in future work for multi-

variate statistical or machine-learning analyses to identify structure–permeability relationships among phytochemicals. Such analyses will enhance the predictive utility of this dataset and support rational compound screening and formulation design.

Multivariate analysis of physicochemical determinants of permeability

To further elucidate the interrelationships among physicochemical parameters and permeability indices, a principal component analysis (PCA) was performed based on ten variables: recovery (AP → BL), AP → BL transport (%), BL → AP transport (%), $P_{app\ (AP\rightarrow BL)}$, $P_{app\ (BL\rightarrow AP)}$, efflux ratio, topological polar surface area (TPSA), number of hydrogen bond donors (HBD), number of hydrogen bond acceptors (HBA), and lipophilicity ($X\log P$). As shown in Fig. 1, the first two principal components (PC1 and PC2) explained 37.2% and 26.6% of the total variance, respectively. The PCA biplot illustrated distribution patterns among compounds, suggesting that permeability-related behavior may be associated with underlying physicochemical properties.

Variables such as $P_{app\ (AP\rightarrow BL)}$, AP → BL transport, and $X\log P$ were positioned in the positive PC1 region, suggesting an overall association with higher permeability-related parameters and transcellular transport characteristics. Conversely, TPSA, HBD, and HBA were negatively loaded on PC1 and positively on PC2, suggesting a potential inverse relationship with permeability-related parameters and reflecting their roles as polarity-related descriptors. Within the analyzed 162 phytochemicals, compounds such as Harmine and Piperine were positioned in the positive PC1 region, characterized by high $P_{app\ (AP\rightarrow BL)}$ values ($\geq 18 \times 10^{-6}$ cm s^{-1}) and elevated $X\log P$ (>3.0), together with low TPSA and limited hydrogen-bonding capacity. These physicochemical profiles are generally associated with higher apparent permeability and may reflect favorable characteristics for transcellular transport. The efflux ratio (ER) and BL → AP transport were oriented in opposite directions along both PC1 and PC2, suggesting a potential inverse relationship between these parameters. In the PCA space, ER and BL → AP transport were oriented in opposite directions, suggesting a directional transport imbalance among certain compounds rather than a simple proportional relationship between these parameters. Compounds such as jatrorrhizine chloride, cromolyn sodium salt, hematoxylin hydrate, icariin, and wogonoside exhibited high efflux ratios (ER ≥ 1.6) but markedly low BL → AP transport (<1.5%). These characteristics

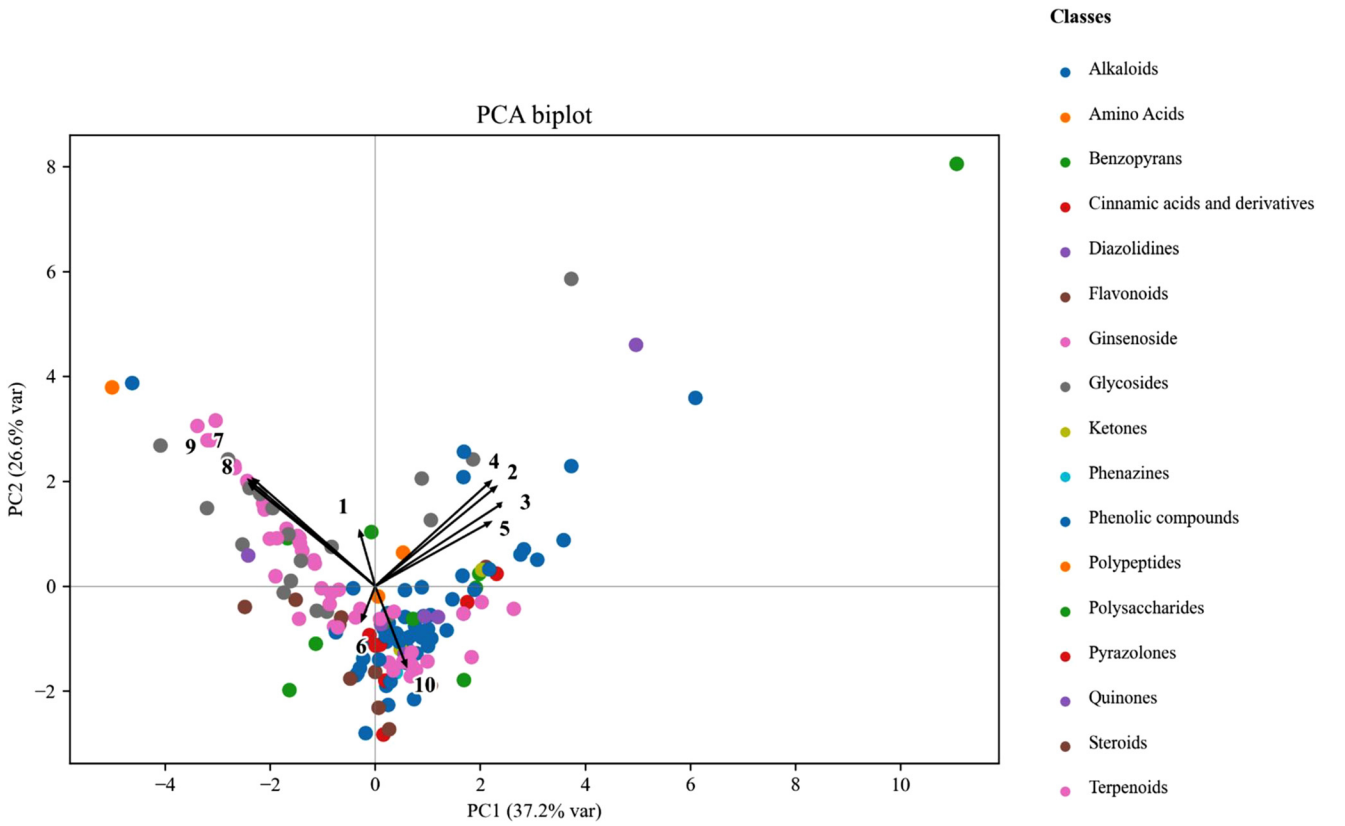

Fig. 1 Principal component analysis (PCA) biplot of 162 phytochemicals based on physicochemical descriptors and permeability-related variables. The biplot integrates both compound distribution (scores) and variable contribution vectors (loadings). PC1 and PC2 explain 63.8% of the total variance. PCA was used as an exploratory multivariate tool to visualize overall associations among variables rather than to infer causality. Numbers (1–10) correspond to: (1) recovery (AP → BL) (%), (2) AP → BL transport (%), (3) BL → AP transport (%), (4) $P_{app\ (AP\rightarrow BL)}$, (5) $P_{app\ (BL\rightarrow AP)}$, (6) efflux ratio, (7) TPSA ($Å^2$), (8) HBD, (9) HBA, and (10) $X\log P$. Colored points represent chemical classes, and arrows indicate the contribution vectors of each variable.

place them opposite to the ER and BL → AP vectors, suggesting a potential inverse relationship between ER and BL → AP transport. This pattern may reflect efflux-related transport behavior, particularly for compounds with higher polarity and lower lipophilicity.

In the PCA biplot (Fig. 1), compounds belonging to alkaloids, benzopyrans, flavonoids, and phenolic compounds tended to distribute toward the positive PC1 region, generally corresponding to higher P_{app} values and moderate lipophilicity. Representative examples include Harmine and Piperine, which exhibited relatively high P_{app} ($\geq 18 \times 10^{-6}$ cm s^{-1}) and $X \log P > 3.0$, suggesting favorable characteristics for transcellular transport. In contrast, ginsenosides, polysaccharides, and polypeptides were distributed toward the negative PC1 region, represented by Icariin and Wogonoside (TPSA > 170 $Å^2$), reflecting their relatively high polarity and physicochemical characteristics associated with lower apparent permeability. The loading patterns in the PCA biplot (Fig. 1) indicated that permeability-related variables (P_{app} and recovery) were primarily aligned with PC1, whereas polarity-related descriptors (TPSA, HBD, and HBA) were more closely associated with PC2. Additionally, the Pearson correlation heatmap of raw features (Fig. 2) further supported these relationships, revealing strong positive correlations among permeability indices (P_{app}, AP → BL, and recovery) and pronounced negative correlations between permeability parameters and polarity-related descriptors (TPSA, HBD, and HBA).

Collectively, the PCA and correlation heatmap provide an exploratory overview of multivariate associations, suggesting that permeability-related parameters appeared to align with lipophilicity and oppose polarity-related descriptors within this dataset.

Examination of PCA loadings revealed that lipophilicity ($X \log P$) contributed most strongly to the first principal component, while polarity descriptors (TPSA, HBD, HBA) loaded negatively. This pattern suggests that molecular hydrophobicity and hydrogen-bonding capacity may represent important contributing factors within this dataset. Compounds with moderate lipophilicity and low polar surface area tended to exhibit higher P_{app} values and improved transcellular diffusion, which aligns with previous reports indicating that optimal absorption occurs in molecules with intermediate $\log P$ (1–3) and limited hydrogen-bonding capacity.[64,65] Conversely, high TPSA and strong hydrogen-bonding potential

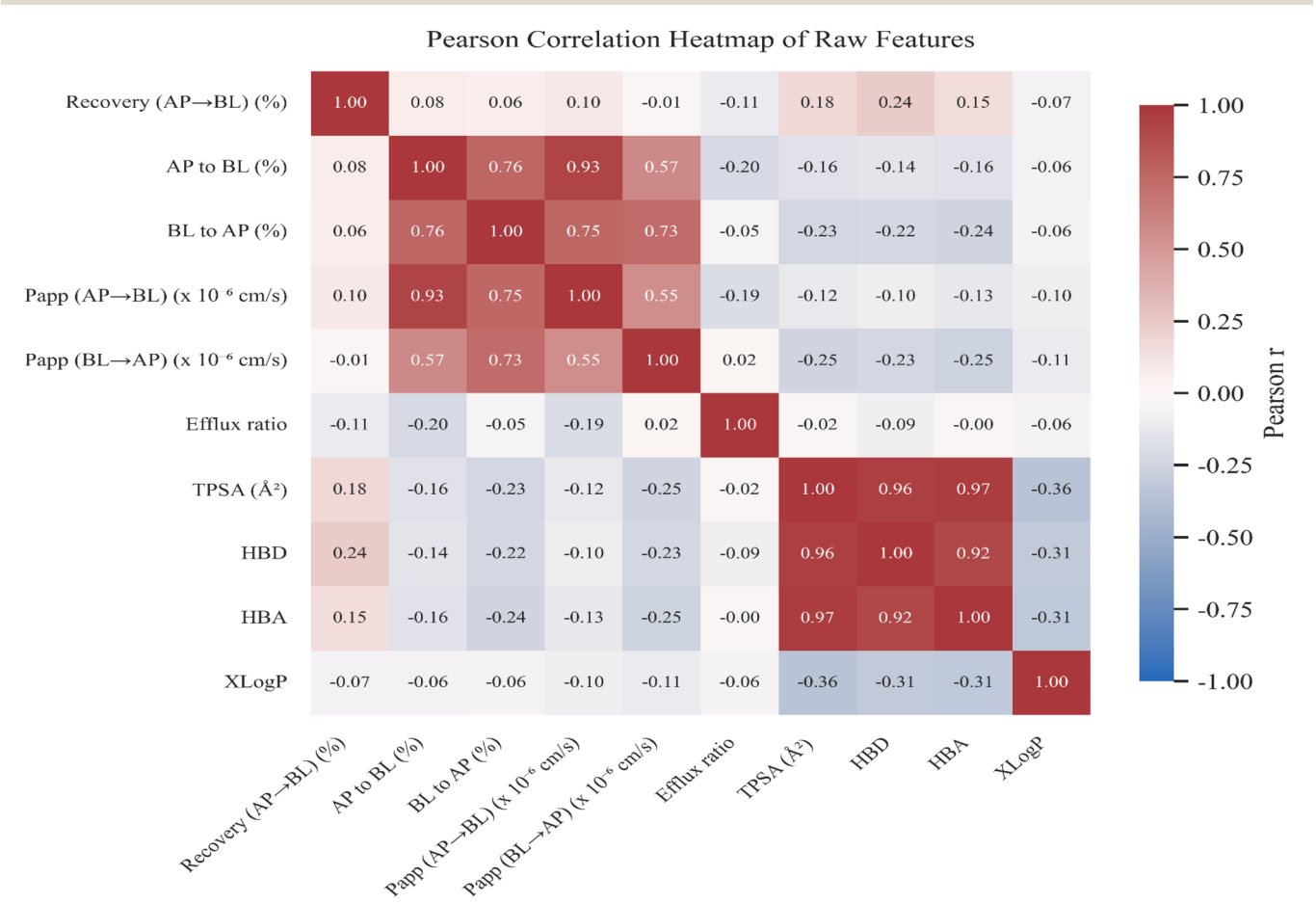

Fig. 2 Pearson correlation heatmap of ten physicochemical and permeability-related variables (recovery, AP → BL, BL → AP, P_{app}, efflux ratio, TPSA, HBD, HBA, $X \log P$, *etc.*) showing the linear interrelationships among parameters in 162 phytochemicals. Positive and negative correlations are indicated by red and blue colors, respectively.

reduce passive diffusion by limiting membrane partitioning.[66,67]

These findings are consistent with Lipinski's "Rule of Five", which predicts that excessive polarity or hydrogen-bond donors/acceptors decrease oral absorption.[68] Similar PCA-based analyses have shown that molecular polarity and surface area are critical determinants of intestinal transport in both natural products and small-molecule drugs.[69,70] Collectively, the current study extends these concepts to structurally diverse phytochemicals, supporting the notion that moderate hydrophobicity and limited hydrogen-bonding favor epithelial permeability, whereas highly polar or glycosylated compounds exhibit restricted transcellular diffusion.

Conclusions

This study systematically characterized the intestinal transport behavior of 162 structurally diverse phytochemicals using a validated HPLC-UV/ELSD analytical platform combined with the Caco-2 cell monolayer model. The results revealed pronounced class- and compound-dependent variations in bioavailability indicators, including transepithelial electrical resistance (TEER), apparent permeability coefficient (P_{app}), and efflux ratio (ER). Notably, cinnamic acids and ketones tended to enhance epithelial barrier integrity, whereas alkaloids, terpenoids, and steroids predominantly weakened it. In terms of permeability, several alkaloids, benzopyrans, flavonoids, glycosides, and phenolic compounds exhibited high P_{app} values consistent with previously reported *in vivo* absorption correlations, while ginsenosides, polypeptides, and polysaccharides remained largely undetectable. Compounds such as piperine and quinidine displayed high permeability yet efflux-prone behavior (ER > 2), highlighting the contribution of transporter-mediated mechanisms.

This study provides a quantitative dataset of 162 phytochemicals, revealing systematic variations in intestinal permeability associated with molecular structure and polarity. Given the triplicate experimental design, the compound-level results should be viewed as exploratory indicators. Even so, the integrated analysis provides a comparative *in vitro* reference framework for evaluating permeability-related behavior relevant to oral absorption and supports hypothesis generation for structure–permeability relationships. In this study, multivariate analysis suggested that permeability variation was broadly associated with lipophilicity ($X \log P$) and molecular polarity (TPSA, HBD, and HBA), consistent with classical absorption-related physicochemical trends described by Lipinski and Veber. PCA was used as an exploratory multivariate tool to visualize overall relationships among variables, and the conclusions of this study are based primarily on direct permeability measurements and correlation analyses. Subsequent studies incorporating transporter inhibition assays, metabolic characterization, and extended replicates will be essential to validate and expand these observations toward the rational development of bioavailable phytochemicals and functional food components.

Conflicts of interest

There are no conflicts of interest to declare.

Data availability

The data that support the findings of this study are not openly available due to reasons of sensitivity and are available from the corresponding author upon reasonable request.

Supplementary information (SI) is available. See DOI: https://doi.org/10.1039/d5fo05099e.

Acknowledgements

This work was supported by an intramural research grant from Korea Institute of Science and Technology (26E0261).

References

1 M. Stielow, A. Witczyńska, N. Kubryń, Ł. Fijałkowski, J. Nowaczyk and A. Nowaczyk, The bioavailability of drugs—the current state of knowledge, *Molecules*, 2023, **28**, 8038.
2 S. H. Thilakarathna and H. V. Rupasinghe, Flavonoid bioavailability and attempts for bioavailability enhancement, *Nutrients*, 2013, **5**, 3367–3387.
3 B. Holst and G. Williamson, Nutrients and phytochemicals: from bioavailability to bioefficacy beyond antioxidants, *Curr. Opin. Biotechnol.*, 2008, **19**, 73–82.
4 M. J. Rein, M. Renouf, C. Cruz-Hernandez, L. Actis-Goretta, S. K. Thakkar and M. da Silva Pinto, Bioavailability of bioactive food compounds: A challenging journey to bioefficacy, *Br. J. Clin. Pharmacol.*, 2013, **75**, 588–602.
5 R. Cong, J.-W. Kim, N.-Y. Lee, Y.-S. Chun, J.-K. Kim, B.-K. Kim, S.-B. Hong and S.-M. Shim, Oral bioavailability enhancement of MK-7 from natto extract via HyperCelle nanoencapsulation in a clinical study, *Appl. Biol. Chem.*, 2025, **68**, 65.
6 N. A. Durán-Iturbide, B. I. Díaz-Eufracio and J. L. Medina-Franco, In silico ADME/Tox profiling of natural products: A focus on BIOFACQUIM, *ACS Omega*, 2020, **5**, 16076–16084.
7 C. B. Aware, D. N. Patil, S. S. Suryawanshi, P. R. Mali, M. R. Rane, R. G. Gurav and J. P. Jadhav, Natural bioactive products as promising therapeutics: A review of natural product-based drug development, *S. Afr. J. Bot.*, 2022, **151**, 512–528.
8 T. Zeng, J. Li and R. Wu, Natural Product Databases for Drug Discovery: Features and Applications, *Pharm. Sci. Adv.*, 2024, 100050.
9 Y. J. Kim, H. Y. Kim, J. D. Lee, H. Y. Kim, J.-E. Im and K.-B. Kim, Analytical method development and dermal absorption of gallic acid, a hair dye ingredient, *Toxicol. Res.*, 2024, **40**, 449–456.
10 C. Barba-Ostria, S. E. Carrera-Pacheco, R. Gonzalez-Pastor, J. Heredia-Moya, A. Mayorga-Ramos, C. Rodríguez-Pólit,

J. Zúñiga-Miranda, B. Arias-Almeida and L. P. Guamán, Evaluation of biological activity of natural compounds: current trends and methods, *Molecules*, 2022, **27**, 4490.
11 T. T. Cushnie, B. Cushnie and A. J. Lamb, Alkaloids: An overview of their antibacterial, antibiotic-enhancing and antivirulence activities, *Int. J. Antimicrob. Agents*, 2014, **44**, 377–386.
12 A. Dey and A. Mukherjee, in *Discovery and development of neuroprotective agents from natural products*, Elsevier, 2018, 237–320.
13 G. Wu, Functional amino acids in growth, reproduction, and health, *Adv. Nutr.*, 2010, **1**, 31–37.
14 X. Kong, B. Tan, Y. Yin, H. Gao, X. Li, L. A. Jaeger, F. W. Bazer and G. Wu, L-Arginine stimulates the mTOR signaling pathway and protein synthesis in porcine trophectoderm cells, *J. Nutr. Biochem.*, 2012, **23**, 1178–1183.
15 X. Liu, Y. Zhang, Y. Zou, C. Yan and J. Chen, Recent advances and outlook of benzopyran derivatives in the discovery of agricultural chemicals, *J. Agric. Food Chem.*, 2024, **72**, 12300–12318.
16 A. Bermejo, A. Collado, I. Barrachina, P. Marqués, N. E. Aouad, X. Franck, F. Garibotto, C. Dacquet, D. H. Caignard and F. D. Suvire, Polycerasoidol, a natural prenylated benzopyran with a dual PPARα/PPARγ agonist activity and anti-inflammatory effect, *J. Nat. Prod.*, 2019, **82**, 1802–1812.
17 N. Ruwizhi and B. A. Aderibigbe, Cinnamic acid derivatives and their biological efficacy, *Int. J. Mol. Sci.*, 2020, **21**, 5712.
18 S. Adisakwattana, Cinnamic acid and its derivatives: mechanisms for prevention and management of diabetes and its complications, *Nutrients*, 2017, **9**, 163.
19 K. E. Heim, A. R. Tagliaferro and D. J. Bobilya, Flavonoid antioxidants: chemistry, metabolism and structure-activity relationships, *J. Nutr. Biochem.*, 2002, **13**, 572–584.
20 A. N. Panche, A. D. Diwan and S. R. Chandra, Flavonoids: an overview, *J. Nutr. Sci.*, 2016, **5**, e47.
21 X. Y. Leong, P. V. Thanikachalam, M. Pandey and S. Ramamurthy, A systematic review of the protective role of swertiamarin in cardiac and metabolic diseases, *Biomed. Pharmacother.*, 2016, **84**, 1051–1060.
22 L. P. Christensen, Ginsenosides: chemistry, biosynthesis, analysis, and potential health effects, *Adv. Food Nutr. Res.*, 2008, **55**, 1–99.
23 A. F. Majdalawieh, M. Massri and G. K. Nasrallah, A comprehensive review on the anti-cancer properties and mechanisms of action of sesamin, a lignan in sesame seeds (Sesamum indicum), *Eur. J. Pharmacol.*, 2017, **815**, 512–521.
24 T. Franza and P. Gaudu, Quinones: more than electron shuttles, *Res. Microbiol.*, 2022, **173**, 103953.
25 M. Ghoneum and A. Jewett, Production of tumor necrosis factor-alpha and interferon-gamma from human peripheral blood lymphocytes by MGN-3, a modified arabinoxylan from rice bran, and its synergy with interleukin-2 in vitro, *Cancer Detect. Prev.*, 2000, **24**, 314–324.
26 V. M. Dembitsky, Biological activity and structural diversity of steroids containing aromatic rings, phosphate groups, or halogen atoms, *Molecules*, 2023, **28**, 5549.
27 A. Ludwiczuk, K. Skalicka-Woźniak and M. Georgiev, *Pharmacognosy*, Elsevier, 2017, pp. 233–266.
28 R. Dhayakaran, S. Neethirajan and X. Weng, Investigation of the antimicrobial activity of soy peptides by developing a high throughput drug screening assay, *Biochem. Biophys. Rep.*, 2016, **6**, 149–157.
29 P. Artursson and J. Karlsson, Correlation between oral drug absorption in humans and apparent drug permeability coefficients in human intestinal epithelial (Caco-2) cells, *Biochem. Biophys. Res. Commun.*, 1991, **175**, 880–885.
30 D. P. Patnana, R. P. Biswal, R. B. Dandamudi, C. S and M. Pandey, Simple HPLC-DAD-based method for determination of ergosterol content in lichens and mushrooms, *J. Liq. Chromatogr. Relat. Technol.*, 2021, **44**, 229–234.
31 Ž Temova and R. Roškar, Stability-indicating HPLC–UV method for vitamin D3 determination in solutions, nutritional supplements and pharmaceuticals, *J. Chromatogr. Sci.*, 2016, **54**, 1180–1186.
32 X.-H. Xu, Q. Su and Z.-H. Zang, Simultaneous determination of oleanolic acid and ursolic acid by RP-HPLC in the leaves of Eriobotrya japonica Lindl, *J. Pharm. Anal.*, 2012, **2**, 238–240.
33 J. Galvao, B. Davis, M. Tilley, E. Normando, M. R. Duchen and M. F. Cordeiro, Unexpected low–dose toxicity of the universal solvent DMSO, *FASEB J.*, 2014, **28**, 1317–1330.
34 N. Kar, D. Gupta and J. Bellare, Ethanol affects fibroblast behavior differentially at low and high doses: A comprehensive, dose-response evaluation, *Toxicol. Rep.*, 2021, **8**, 1054–1066.
35 L. Jamalzadeh, H. Ghafoori, R. Sariri, H. Rabuti, J. Nasirzade, H. Hasani and M. R. Aghamaali, Cytotoxic effects of some common organic solvents on MCF-7, RAW-264.7 and human umbilical vein endothelial cells, *Avicenna J. Med. Biochem.*, 2016, **4**, 10–33453.
36 A. Kourkopoulos, D. T. Sijm, J. Geerken and M. F. Vrolijk, Compatibility and interference of food simulants and organic solvents with the in vitro toxicological assessment of food contact materials, *J. Food Sci.*, 2025, **90**, e17659.
37 R. Konsoula and F. A. Barile, Correlation of in vitro cytotoxicity with paracellular permeability in Caco-2 cells, *Toxicol. in Vitro*, 2005, **19**, 675–684.
38 J.-h. Hwang, J.-h. Hong and K.-M. Lim, Investigation of alternative cell models to BALB/c 3T3 for in vitro neutral red uptake phototoxicity test of pharmaceuticals: NIH 3T3 and HaCaT cells, *Toxicol. Res.*, 2025, 1–11.
39 C. M. Peters, R. J. Green, E. M. Janle and M. G. Ferruzzi, Formulation with ascorbic acid and sucrose modulates catechin bioavailability from green tea, *Food Res. Int.*, 2010, **43**, 95–102.
40 N.-H. Truong, S. Lee and S.-M. Shim, Screening bioactive components affecting the capacity of bile acid binding and pancreatic lipase inhibitory activity, *Appl. Biol. Chem.*, 2016, **59**, 475–479.

41 E.-H. Choi, D.-Y. Lee, S. Kim, J.-O. Chung, J.-K. Choi, K.-M. Joo, H. W. Jeong, J. K. Kim, W. G. Kim and S.-M. Shim, Influence of flavonol-rich excipient food (onion peel and Dendropanax morbifera) on the bioavailability of green tea epicatechins in vitro and in vivo, *Food Funct.*, 2017, **8**, 3664–3674.

42 I. T. Jolliffe and J. Cadima, Principal component analysis: a review and recent developments, *Phil. Trans. R. Soc. A-Math. Phys. Eng. Sci.*, 2016, **374**, 20150202.

43 S. Lee, S. Yang, W.-S. Shim, E. Song, S. Han, S.-S. Park, S. Choi, S. H. Joo, S. J. Park and B. Shin, Development and Validation of an Improved HPLC-MS/MS Method for Quantifying Total and Unbound Lenalidomide in Human Plasma, *Pharmaceutics*, 2024, **16**, 1340.

44 T. Suzuki, Regulation of the intestinal barrier by nutrients: The role of tight junctions, *J. Anim. Sci.*, 2020, **91**, e13357.

45 S. Bernardi, C. Del Bo', M. Marino, G. Gargari, A. Cherubini, C. Andrés-Lacueva, N. Hidalgo-Liberona, G. Peron, R. González-Dominguez and P. Kroon, Polyphenols and intestinal permeability: rationale and future perspectives, *J. Agric. Food Chem.*, 2019, **68**, 1816–1829.

46 T. Shiobara, T. Usui, J. Han, H. Isoda and Y. Nagumo, The reversible increase in tight junction permeability induced by capsaicin is mediated via cofilin-actin cytoskeletal dynamics and decreased level of occludin, *PLoS One*, 2013, **8**, e79954.

47 Y. Tsukura, M. Mori, Y. Hirotani, K. Ikeda, F. Amano, R. Kato, Y. Ijiri and K. Tanaka, Effects of capsaicin on cellular damage and monolayer permeability in human intestinal Caco-2 cells, *Biol. Pharm. Bull.*, 2007, **30**, 1982–1986.

48 Y. Sasaki, H. Tatsuoka, M. Tsuda, T. Sumi, Y. Eguchi, K. So, Y. Higuchi, K. Takayama, Y. Torisawa and F. Yamashita, Intestinal permeability of drugs in caco-2 cells cultured in microfluidic Devices, *Biol. Pharm. Bull.*, 2022, **45**, 1246–1253.

49 G. Camenisch, J. Alsenz, H. van de Waterbeemd and G. Folkers, Estimation of permeability by passive diffusion through Caco-2 cell monolayers using the drugs' lipophilicity and molecular weight, *Eur. J. Pharm. Sci.*, 1998, **6**, 313–319.

50 Å. Sjöberg, M. Lutz, C. Tannergren, C. Wingolf, A. Borde and A.-L. Ungell, Comprehensive study on regional human intestinal permeability and prediction of fraction absorbed of drugs using the Ussing chamber technique, *Eur. J. Pharm. Sci.*, 2013, **48**, 166–180.

51 E. Bechgaard, S. Gizurarson, L. Jørgensen and R. Larsen, The viability of isolated rabbit nasal mucosa in the Ussing chamber, and the permeability of insulin across the membrane, *Int. J. Pharm.*, 1992, **87**, 125–132.

52 I. Hubatsch, E. G. Ragnarsson and P. Artursson, Determination of drug permeability and prediction of drug absorption in Caco-2 monolayers, *Nat. Protoc.*, 2007, **2**, 2111–2119.

53 B. Press and D. D. Grandi, Permeability for intestinal absorption: Caco-2 assay and related issues, *Curr. Drug Metab.*, 2008, **9**, 893–900.

54 M.-K. Choi, S. Jin, J.-H. Jeon, W. Y. Kang, S. J. Seong, Y.-R. Yoon, Y.-H. Han and I.-S. Song, Tolerability and pharmacokinetics of ginsenosides Rb1, Rb2, Rc, Rd, and compound K after single or multiple administration of red ginseng extract in human beings, *J. Ginseng Res.*, 2020, **44**, 229–237.

55 P. Artursson, K. Palm and K. Luthman, Caco-2 monolayers in experimental and theoretical predictions of drug transport, *Adv. Drug Delivery Rev.*, 2012, **64**, 280–289.

56 V. Gupta, N. Doshi and S. Mitragotri, Permeation of insulin, calcitonin and exenatide across Caco-2 monolayers: measurement using a rapid, 3-day system, *PLoS One*, 2013, **8**, e57136.

57 M. F. Fromm, R. B. Kim, C. M. Stein, G. R. Wilkinson and D. M. Roden, Inhibition of P-glycoprotein–mediated drug transport: a unifying mechanism to explain the interaction between digoxin and quinidine, *Circulation*, 1999, **99**, 552–557.

58 R. K. Bhardwaj, H. Glaeser, L. Becquemont, U. Klotz, S. K. Gupta and M. F. Fromm, Piperine, a major constituent of black pepper, inhibits human P-glycoprotein and CYP3A4, *J. Pharmacol. Exp. Ther.*, 2002, **302**, 645–650.

59 Y. Han, T. M. C. Tan and L.-Y. Lim, In vitro and in vivo evaluation of the effects of piperine on P-gp function and expression, *Toxicol. Appl. Pharmacol.*, 2008, **230**, 283–289.

60 M. Estudante, J. G. Morais, G. Soveral and L. Z. Benet, Intestinal drug transporters: an overview, *Adv. Drug Delivery Rev.*, 2013, **65**, 1340–1356.

61 T. Hou, W. Zhang, K. Xia, X. Qiao and X. Xu, ADME evaluation in drug discovery. 5. Correlation of Caco-2 permeation with simple molecular properties, *J. Chem. Inf. Comput. Sci.*, 2004, **44**, 1585–1600.

62 C. A. Lipinski, Lead-and drug-like compounds: the rule-of-five revolution, *Drug Discov. Today Technol.*, 2004, **1**, 337–341.

63 S. Yamashita, T. Furubayashi, M. Kataoka, T. Sakane, H. Sezaki and H. Tokuda, Optimized conditions for prediction of intestinal drug permeability using Caco-2 cells, *Eur. J. Pharm. Sci.*, 2000, **10**, 195–204.

64 D. F. Veber, S. R. Johnson, H.-Y. Cheng, B. R. Smith, K. W. Ward and K. D. Kopple, Molecular properties that influence the oral bioavailability of drug candidates, *J. Med. Chem.*, 2002, **45**, 2615–2623.

65 M. Yazdanian, S. L. Glynn, J. L. Wright and A. Hawi, Correlating partitioning and Caco-2 cell permeability of structurally diverse small molecular weight compounds, *Pharm. Res.*, 1998, **15**, 1490.

66 K. Palm, K. Luthman, J. Ros, J. Gråsjö and P. Artursson, Effect of molecular charge on intestinal epithelial drug transport: pH-dependent transport of cationic drugs, *J. Pharmacol. Exp. Ther.*, 1999, **291**, 435–443.

67 S. Winiwarter, N. M. Bonham, F. Ax, A. Hallberg, H. Lennernäs and A. Karlén, Correlation of human jejunal permeability (in vivo) of drugs with experimentally and theoretically derived parameters, A multivariate data analysis approach, *J. Med. Chem.*, 1998, **41**, 4939–4949.

68 C. A. Lipinski, F. Lombardo, B. W. Dominy and P. J. Feeney, Experimental and computational approaches to estimate solubility and permeability in drug discovery and development settings, *Adv. Drug Delivery Rev.*, 1997, **23**, 3–25.
69 M. Kansy, F. Senner and K. Gubernator, Physicochemical high throughput screening: parallel artificial membrane permeation assay in the description of passive absorption processes, *J. Med. Chem.*, 1998, **41**, 1007–1010.
70 H. Pajouhesh and G. R. Lenz, Medicinal chemical properties of successful central nervous system drugs, *NeuroRx*, 2005, **2**, 541–553.